Conversion of Waste Plastics to Liquid Fuels by Micro-Mesoporous HZSM-5 Catalysts

Dureem Munir
Sheridan College - Davis Campus
Muhammad Rashid Usman (mrusman.icet@pu.edu.pk)
University of the Punjab https://orcid.org/0000-0002-4584-0842

Research Article

Keywords: Zeolite HZSM-5, Micro-mesoporous catalysts, Waste plastic, Chemical recycling, Hydrocracking

Posted Date: March 30th, 2021

DOI: https://doi.org/10.21203/rs.3.rs-343214/v1

Abstract

Three micro-mesoporous HZSM-5 catalysts were synthesized using three different mesoporous templates and studied for the conversion of a model municipal waste plastic mixture to produce liquid fuels of high value. For the comparison, the conversion of an actual waste plastic mixture and HDPE was also studied. The experiments were performed in a batch stirred reactor at three reaction temperatures (350, 375, and 400 °C) and at fixed cold H_2 pressure (20 bar), reaction time (60 min), and plastic to catalyst ratio (20:1 by wt.). The micro-mesoporous catalysts produced better activity and selectivity than their parent HZSM-5 catalyst. The catalyst, prepared by combining two different templates, was found to be the most favorable catalyst offering 67.1% liquid yield at 400 °C with actual waste plastic. The best performing catalyst has shown the prospects for commercial applications.

1. Introduction

The waste generated due to an ever increasing demand of plastic products poses a serious environmental concern. The recycling of plastic waste not only reduces the amount of the waste, but it also exploits the valuable resource of the waste [1–5]. Chemical recycling methods those of thermal cracking or pyrolysis, catalytic cracking, and hydrocracking transform the plastic wastes to liquid and gaseous fuels. Among these cracking methods, hydrocracking is considered the most promising method that in the presence of hydrogen and catalyst produces a high value liquid product containing lower quantities of olefins [6–8]. Moreover, hydrocracking is exothermic and requires lower reaction temperatures [9, 10].

In the literature, the catalytic hydrocracking of a plastic material has been mainly studied over microporous zeolite catalysts [6, 11–26]. Due to the highly acidic nature of the zeolites, they have extremely good cracking ability, however, because of their microporous character, they offer diffusion resistance [27–29] and very high gas yields are resulted [30]. Although gaseous fuels are useful, but they are usually of low value due to their low energy density and high transportation cost [31]. A few investigators have also studied the hydrocracking of plastics over mesoporous and Al-modified mesoporous catalysts [21, 26, 32, 33]. Mesoporous catalysts offer low activity, much lower compared to the microporous zeolites due to their weak acidity [34, 35], however, they allow larger reactant and product molecules to diffuse through their structure which helps in increasing their activity and liquid selectivity. For cracking of plastic molecules where the reactants are large polymeric fragments and the desired product is in the gasoline and diesel range, a micro-mesoporous composite catalyst that has the activity of zeolites and the selectivity of the mesoporous materials will be undoubtedly a better choice.

In our previous works we tested the aluminum-modified mesoporous catalysts [26, 32, 33] as well as the micro-mesoporous USY and beta catalysts [27, 36] for the hydroconversion of a model mixture of plastics. Rather favorable results were achieved with Al-modified SBA catalysts with respect to the catalyst selectivity, however, the activity was not comparable to that of microporous zeolites. With micro-mesoporous USY catalysts, highly promising results were obtained in terms of both the catalyst activity

and selectivity. The results with micro-mesoporous USY catalysts have led us to work with the micro-mesoporous HZSM-5 catalysts.

Zeolite ZSM-5 is a heavily investigated and commercially well-developed zeolite. It is highly active and thermally and hydrothermally stable zeolite that has been widely used in cracking, alkylation, and isomerization reactions. The ZSM-5 catalyst has also been extensively used by the researchers [12–21] for the plastic hydrocracking and it has shown considerably high activity in the cracking reaction. However, the principal drawback of using a ZSM-5 zeolite lies in its small pore size that results in high gas yields. In the present work, in order to exploit the high cracking ability of HZSM-5, micro-mesoporous HZSM-5 catalysts are synthesized, characterized, and their activity, selectivity, and stability are tested in the hydrocracking of a model plastic mixture, real plastic waste, and HDPE. To the best of our knowledge, the micro-mesoporous HZSM-5 catalysts have never been tested for the hydrocracking of plastic materials.

2. Experimental

Catalyst Preparation

16 g of powdered ZSM-5 zeolite (CBV2314, Zeolyst International) was mixed with 1.5 M NaOH solution. The zeolite ZSM-5 was in the ammonium form therefore it was calcined previously for five hours at 600°C (heating rate of 2°C/min) to obtain the proton form. The alkali solution was then allowed to agitate at 40°C for 30 min. 16 g of tetraethylorthosilicate (TEOS, 98.0%, Sigma-Aldrich) was then added into this solution and the matter was allowed to stir for four hours at 35°C. Separately, 7 g of P123 (Sigma-Aldrich) was mixed into 1 M HCl, and the mixture was stirred for four hours until the contents were completely mixed. 0.1 g NH_4F (≥ 98.0%, Sigma-Aldrich) was then added and stirring was carried out for further 30 min. The two mixtures were combined, and the final mixture was stirred for 24 h at 40°C. Here the mixture had pH value of 1. The mixture was then hydrothermally crystallized in a Teflon lined SS autoclave at 110°C for 24 h. The resulting crystallized material was washed many times with doubly distilled water and centrifuged, and the final catalyst was dried at 100°C for 20 h and then calcined for 5 h at 600°C. The heating rate to reach at the calcination temperature was ~ 2°C/min. The ion-exchange was carried out to convert the sodium form to the H form of the catalyst. This was followed by filtration, washing, drying for 12 h at 100°C, and calcination in air at 600°C for 4 h. The resultant catalyst was identified as ZC-P. ZC-F and ZC-FP were prepared following the same method, but using F127 (Sigma-Aldrich) and the mixture of P123 and F127, respectively as the template material.

Catalyst Characterization

The SEM micrographs of the synthesized catalysts were acquired by Mira 3 TESCAN Field Emission Scanning Electron Microscope. Carbon sputtering of the catalysts was performed before taking the images. Micromeritics TriStar II-3020 was employed for N_2-BET analysis. Small angle XRD of the catalysts was performed using PANanalytical Empyrean diffractometer (Cu-Kα X-ray radiations) whereas

PANalytical X'Pert diffractometer was employed for the wide angle XRD. Infrared (IR) and Py-IR spectra of the catalysts were acquired by JASCO, FTIR-4100. Pyridine (≥ 99.0%) was obtained from Sigma-Aldrich. For the FTIR analysis, KBr pellets consisting of 98wt% of KBr and 2wt% catalyst were employed. Py-FTIR analysis was employed to observe the character of the acid sites.

Catalytic Experiments

The activity and selectivity performance of the synthesized catalysts were tested by carrying out the hydroconversion or hydrocracking reactions of a model waste plastic mixture, HDPE, and an actual waste plastic mixture. The model plastic mixture was prepared by mixing virgin 40wt% HDPE (ρ = 0.95 g/cm^3), 10wt% LDPE (ρ = 0.92 g/cm^3, MP = 100–125°C), 30wt% PP (M = 250,000 g/mol, ρ = 0.90 g/cm^3), and 20wt% PS (M = 192,000 g/mol). All the virgin plastics were obtained from Sigma-Aldrich. Waste plastics mixture consisted of 40wt% HDPE (H&S shampoo bottles washed, cleaned, and dried), 10wt% LDPE (unused plastic bags used for shopping), 30wt% PP (unused boxes used for takeaways), and 20wt% PS (unused tea cups), all were procured from the local market.

A 500 ml batch stirred reactor (Parr Instrument Co.) was used to perform the catalytic experiments. The full detail of the experimental system is available in Munir [37]. For each experiment, 10 g plastic along with 0.5 g catalyst was charged to the reactor and hydrogen pressure of 20 bar at initial cold conditions was provided. The reactor was heated at the rate of 4.6°C/min to reach at the set reaction temperature where a 60 min holding time was supplied. After the completion of the reaction, the reactor was cooled down to the ambient conditions and the products were collected and analyzed. Figure 1 shows the analysis scheme followed in the analysis of the products. The reactor contents were subjected to n-heptane (≥ 99.0% purity, Sigma-Aldrich) extraction. The n-heptane soluble fraction was designated as the "oil yield". The raffinate was mixed with tetrahydrofuran (THF, ≥ 99.0% purity, Sigma-Aldrich) and the combined yield of the n-heptane soluble fraction and the THF soluble fraction was named as "liquid yield". The solid residuum containing the unconverted plastic, coke formed during the reaction, and the used catalyst was dried at 110°C for several hours and weighed. The experimental conversion for the reaction was calculated based on this dried residuum. The gas yield was found by subtracting the weight of the reactor at the end of an experiment after relieving the gases from the weight of the reactor taken at the beginning, before pressurizing the reactor with H_2 gas. To find out the amounts of C5-C12 (gasoline), C13-C18 (diesel), and C19 + fraction, the oil fraction was further analyzed by GC-FID (Shimadzu GC-2014). The GC was installed with a 30 m long and 0.25 mm inner diameter capillary column (Agilent DB-1MS).

3. Results And Discussion

3.1 Characterization

The surface morphology of each of the catalysts is given by the SEM images displayed in Fig. 2. The commercial HZSM-5 catalyst (CBV2314) presents small cubic-shaped crystals that represent the

characteristic HZSM-5 structure [38, 39]. The SEM micrographs of ZC-P display cubic HZSM-5 crystals present uniformly with the fibrous transparent worm like structures, the defining characteristic of SBA-15 [40]. The SEM images of ZC-F show the presence of cubic crystals of ZSM-5 along with some spherical shaped particles that represent the presence of SBA-16 mesoporous content as it is synthesized with F-127 as the template. There is no phase segregation that represents the presence of uniform micro-mesoporous structure. For the ZC-FP, the SEM micrographs show the presence of cubic crystals of HZSM-5 along with the spherical particles of SBA-16 together with the transparent loose aggregates of SBA-15. The catalyst displays the co-existence of the cubic and hexagonal mesoporous phase along with microporous crystals of HZSM-5. The overall morphology of the micro-mesoporous catalysts is highly coarse compared to the HZSM-5 catalyst. The desilication process used in the synthesis of the micro-mesoporous catalysts resulted in the formation of coarse texture in these catalysts [41].

Transmission Electron Microscopy (TEM) images of the investigated catalysts show the highly porous structure of the catalysts. For the HZSM-5 catalyst (Fig. 3a), the lattice fringes reveal the crystalline morphology and that the nanopores are arranged in a regular array. Figure 3b shows the TEM image of ZC-F, taken perpendicular to the pore direction, reveals the large pore cage-like matrix structure. These cage-like structures represent cubic *Im*3*m* structure [42] that forms SBA-16 mesoporous composite of ZSM-5 in ZC-F. The TEM image of ZC-FP is shown in Fig. 3c. The image shows heterogeneity caused by the presence of different types of structures. This signifies the use of two different templates in the preparation of ZC-FP catalyst. Figure 3d shows the TEM image of the ZC-P catalyst. The image presents the uniform large channel structure of SBA-15 along the axis of the pores. The dark gray structure indicates the microporous region of ZSM-5 catalyst. The TEM images confirm the micro-mesoporous nature of all the three catalysts.

The surface characteristics of the catalysts based on the N_2-BET measurements are given in Table 1. It is found that the surface areas of all the micro-mesoporous catalysts are higher as compared to the HZSM-5 catalyst with the highest in the case of ZC-P. The highest mesoporous area is present in ZC-F.

Table 1
Structural properties of the micro-mesoporous HZSM-5 catalysts

Catalyst	Si/Al ratio by EDX	S_{BET}[a] (m^2/g)	S_{micro}[b] (m^2/g)	S_{meso}[c] (m^2/g)	v_{total}[d] (cm^3/g)	v_{micro}[b] (cm^3/g)	v_{meso}[e] (cm^3/g)	d_{meso}[e] (nm)
HZSM-5	13.56	339.2	283.5	55.7	0.150	0.127	0.023	3.24
ZC-F	34.56	364.2	162.6	201.6	0.188	0.068	0.12	6.52
ZC-FP	33.98	370.8	184.3	186.5	0.178	0.078	0.10	6.53
ZC-P	31.21	382.5	208.4	174.1	0.284	0.094	0.19	6.65

[a] surface area by using BET method, [b] obtained by *t*-plot, [c] $S_{BET} - S_{micro}$, [d] $v_{micro} + v_{meso}$,

[e] *BJH* adsorption method

The small angle X-ray diffraction patterns of the catalysts are shown in Fig. 4. ZC-P catalyst displays three well resolved peaks at 2θ value of 0.97, 1.64, and 1.88 that are attributed to (100), (110), and (200) reflections, respectively [40, 45]. Well-ordered hexagonal mesoporous structure with *P*6*mm* symmetry is found in this composite catalyst. X-ray diffraction pattern of ZC-F presents three peaks at 2θ value of 0.73, 1.11, and 1.23 that indicate (110), (200), and (211) planes, respectively [46, 47]. However the latter two peaks are clearly tiny and difficult to differentiate and therefore not well resolved. This shows the formation of low order mesostructure [48, 49]. The catalyst ZC-FP displays a sharp peak at 2θ value of 0.68 with a tiny shoulder peak at 0.74 assigned to (100) and (110) reflections, respectively [40, 45–47]. Again a low order mesostructure is the result. This might be attributed to the co-existence of cubic and hexagonal mesostructures in the same catalyst.

The XRD patterns of all the four catalysts, in the wide-angle range, are presented in Fig. 5. HZSM-5 shows well resolved sharp peaks that show highly crystalline structure of HZSM-5. The diffractograms of the micro-mesoporous catalysts show that the crystallinity of the HZSM-5 is retained after the alkaline treatment. However, with the introduction of mesoporosity, there is observed a decrease in crystallinity in the composite catalysts. Among the three micro-mesoporous catalysts, the crystalline behavior of ZC-P is observed to be the closest to the parent HZSM-5 catalyst. This observation may be caused by the nature of the template used in the synthesis of ZC-P.

3.2 Hydrocracking Performance of the Catalysts

3.2.1 Hydrocracking of Model Waste Plastic Mixture

Figure 6 shows the results of the catalytic hydrocracking experiments over HZSM-5 and its micro-mesoporous catalysts. At the reaction temperature of 350°C, all the micro-mesoporous catalysts produced higher conversion and yield of the liquid products than that produced over the parent HZSM-5 catalyst. The HZSM-5 catalyst, on the other hand, delivered higher gas yield. The reason for these

observations might be attributed to the improved diffusion of the large polymeric molecules to the active sites due to the presence of mesopores in the micro-mesoporous catalysts. The mesopores also allowed the larger liquid molecules formed to diffuse out of the catalyst pores without further cracking to cause higher yield of the liquid product. The small micropores in HZSM-5 hindered the diffusion of large liquid molecules, therefore, the large molecules were cracked and kept on cracking into small enough molecules to leave the catalyst pores. The HZSM-5 catalyst, therefore, yielded the increased amount of gaseous content. Among the micro-mesoporous composite catalysts, ZC-P with the highest microporous area as compared to the other composite catalysts yielded the highest conversion and considerable amount of gaseous product whereas the highest liquid yield and the least gaseous product were obtained over ZC-FP. ZC-FP catalyst is expected to have the combination of both the hexagonal and cubic pore arrangement, the combination might have improved the diffusion for large molecular weight product. Additionally, all the micro-mesoporous HZSM-5 catalysts are found to exhibit more acid sites as compared to the parent HZSM-5 catalyst. Therefore, higher acid sites are present in these catalysts and as a result they produced higher conversion than that of the parent HZSM-5 catalyst even at the lowest reaction temperature of 350°C.

At 375°C, again all the micro-mesoporous catalysts provided increased conversion and liquid selectivity, but decreased amount of gaseous products compared to their parent HZSM-5 catalyst. Both ZC-P and ZC-FP offered virtually the same conversion, however, ZC-FP provided greater selectivity of liquid product and lesser amount of gases. The increased micropore volume of ZC-P might be the cause of its increased gas yield and decreased liquid selectivity.

At the highest reaction temperature, 400°C, all the catalysts came up with the same activity performance giving virtually the same conversion. It might be happened due to the increased thermal energy provided at this high temperature [50–54]. Again, ZC-FP catalyst provided the increased liquid yield and the decreased gas selectivity, in contrast to, the HZSM-5 catalyst which delivered the lowest liquid yield and the highest gas selectivity.

The results of the gas chromatographic analysis for the oil fraction are given in Fig. 7. At 350°C, the highest amount of gasoline is obtained from the HZSM-5 catalyst. The shape selectivity of HZSM-5 allowed to produce the lighter liquid in greater amount. The light diesel and heavy diesel products underwent cracking in order to leave the small pores of the catalyst. Among the micro-mesoporous catalysts, ZC-P produced the largest amount of gasoline closely followed by ZC-FP. ZC-P contains better micropore volume which might be the reason for its increased gasoline content. ZC-FP and ZC-F are found more selective towards diesel fraction. At 375°C, both ZC-FP and HZSM-5 catalysts are proved highly selective towards gasoline. ZC-FP produced gasoline at the expense of light diesel, i.e., the light diesel fraction of ZC-FP at higher temperature underwent further cracking to produce gasoline fraction. Again at 400°C, HZSM-5 and ZC-FP are found highly selective towards gasoline where the light and heavy diesel fractions of ZC-FP are converted to the increased gasoline amount in the product. With ZC-P when compared to the results at 375°C, at this temperature, both the gasoline and light diesel fractions are increased with a decrease in heavy diesel fraction.

3.2.2 Hydrocracking of HDPE

HDPE is selected as feed for further testing of the catalysts as it is the most difficult plastic to be cracked among the plastics present in the municipal waste. Hydrocracking reactions of HDPE are performed at 400°C, 60 min residence time, 20 bar cold H_2 pressure, and 20:1 (by wt.) plastic to catalyst ratio. Figure 8a shows the conversion and selectivity of the products obtained during the hydrocracking of HDPE. It is observed that ~ 100% conversion is obtained over all the catalysts. The increased oil yield (49.7%) and liquid yield (50.1%) and the decreased gas yield are produced by ZC-F catalyst. On the contrary, the lowest oil and liquid yield and the highest gas yield are produced over the HZSM-5 catalyst. The amount of liquid product is decreased whereas the gas yield is increased in the order of HZSM-5 > ZC-P > ZC-FP > ZC-F.

Under the same reaction conditions, it is found that for all the catalysts, the hydrocracking reactions with HDPE result nearly the same conversion, lower amount of liquid yield, and significantly higher gas yield compared to their corresponding reactions with the model plastic mixture (Fig. 8c). This is reasonable and can be explained on the basis that the model mixture contains significant amounts of PS, PP, and LDPE which are expected to yield higher liquid products. Moreover, the interaction among the various plastics can result in the formation of higher liquid content obtained with the hydrocracking of the model plastic mixture [55]. Among the micro-mesoporous catalysts, the performance of ZC-FP is appeared to be affected most.

The gas chromatographic analysis of the heptane solubles, i.e., oil obtained with HDPE is shown in Fig. S1a (in the supplementary material). It is observed that the product obtained over all the catalysts is majorly selective towards gasoline. The ZC-P catalyst produced the highest gasoline fraction of 84.0%, followed, respectively, by HZSM-5, ZC-FP, and BC-27. When compared to the gasoline yield for the model plastic mixture under the same reaction conditions (Fig. S1c), it is found that the gasoline component for the model plastic mixture and HDPE is nearly the same over HZSM-5 and ZC-FP. However, ZC-P produced greater amount of gasoline with HDPE and the amount of gasoline is increased from 73.5–84.0%.

3.2.3 Hydrocracking of Actual Waste Plastic Mixture

Figure 8 also displays the outcome of the hydrocracking reactions with actual waste plastic mixture at 400°C reaction temperature. It is found that the maximum conversion of waste plastic mixture is obtained with ZC-F though only marginally different to the conversions obtained over HZSM-5, ZC-FP, and ZC-P. Again, the highest gas yield with least amount of liquid product is obtained with HZSM-5. The highest liquid yield of ~ 66.5% and the lowest gas yield of ~ 22% are obtained with ZC-F and ZC-FP. The oil product is decreased in the order of ZC-FP ~ ZC-F□ZC-P > HZSM-5.

Comparing the performance of the catalysts with the model plastic mixture, it is found that all the catalysts showed slightly lower conversion, but increased ratio of liquid or oil yield to gas yield with actual waste plastic mixture, i.e., higher liquid yield and lower gas yield to that of the model plastic mixture. This might be attributed to the presence of some impurities such as detrimental heteroatoms and trace metals in actual waste plastic mixture that interfered with the cracking reaction and engaged

with the highly active sites thus resulted in a decrease in the conversion, reduced gas product, and better liquid yield.

The results of the gasoline selectivity (Fig. S1b) with actual waste plastic mixture reveal that the highest gasoline yield (72.7%) is obtained using ZC-P. The gasoline component decreased in the order ZC-P > HZSM-5□ZC-F□ZC-FP. When compared to the model plastic mixture, Fig. S1c, it is found that all the catalysts produced lower gasoline with actual waste plastic mixture than by the corresponding reactions with the model plastic mixture. This further strengthens the idea of interference of the impurities present in actual waste plastic resulted in inhibiting the effect of highly active sites of the catalysts.

3.2.4 Stability Check of the Catalysts

3.2.4.1 Hydrocracking Reactions over Dried-Spent Catalysts

The stability of the catalysts was analyzed by reutilizing the used or spent catalysts for the hydrocracking of the model waste plastic mixture. The spent catalyst was recovered from an earlier hydrocracking experiment with the model plastic mixture carried out at 400°C. The spent catalyst was then heated and dried at 120°C for 30 min. The dried-spent catalyst was mixed with the fresh catalyst in 1:1 ratio by weight in order to compensate the loss of the used catalyst and to maintain the same feed to catalyst ratio. Figure 9a shows the findings for the hydrocracking reactions over dried-spent catalysts. When compared to the reactions over the fresh catalysts, it is observed that the hydrocracking experiments with dried-spent catalysts yielded nearly the same conversion with HZSM-5 and its composites. The liquid yield is increased considerably with a significant decrease in the gas yield. The highest liquid yield of 79.6% is produced by ZC-FP. This corresponds to the reduction in the elevated cracking ability of the catalysts that might be caused by the coke deposition on the highly active sites of the catalysts, i.e., the highly active sites are rather masked. It is found that the dried-spent catalysts are less selective towards gasoline (Fig. S2a) than their corresponding fresh catalysts. The highest amount of gasoline is produced over HZSM-5 which is 64.2% and the gasoline yield is decreased in the order HZSM-5□ZC-F□ZC-P□BC27.

3.2.4.2 Hydrocracking Reactions over Calcined-Spent Catalysts

The stability of the catalysts was further analyzed by reusing HZSM-5 and its composites for the hydrocracking reactions with the model plastic mixture. This time the spent catalysts were calcined in air in order to remove the carbonaceous material deposited on the catalysts surfaces. The outcome of the hydrocracking reactions over the calcined-spent catalysts is given in Fig. 9a. It is found that all the regenerated materials yielded nearly the same conversion of 100% as that of the fresh catalyst and produced higher gas yield and lower liquid yield. This might be assigned to the increase in the active sites due to the calcination that decomposes the coke deposited on the active sites of the catalysts. Also, some sintering of the particles might have occurred reducing the average pore size of the catalysts thereby generating increased amounts of gases with reduced quantities of liquids. It is, however,

important to mention that the trends of the yields for the various catalysts are remained the same as that obtained with the fresh catalysts.

It is found that all the calcined-spent catalysts have produced less gasoline to their corresponding fresh catalysts and higher gasoline to that of spent catalysts without calcination. The coke removal due to calcination opened up the highly active sites of the micropores to produce more gasoline fraction than that of the dried-spent catalysts. The highest gasoline fraction is produced over HZSM-5 equal to 66.6% followed, respectively, by ZCF, ZC-FP, and ZC-P.

4. Concluding Remarks

The catalysts characterization has confirmed the development of micro-mesoporous HZSM-5 containing mesoporous silica. During the synthesis process, the micro-mesoporous catalysts maintained the microporous crystallinity of HZSM-5. However, the mesoporous character has decreased the intensity of crystallinity.

In the hydrocracking testing of the catalysts with model plastic mixture, the ZC-FP catalyst (prepared using mixture of two templates) is found the best catalyst as, generally, it provided increased conversions and yields of the liquid product with the decreased gaseous components. The n-heptane solubles show that both HZSM-5 and ZC-FP provide the high content of gasoline fraction. However, HZSM-5 due to its microporous nature is found highly selective towards gaseous product.

With HDPE all the catalysts showed nearly the same conversion. The ZC-FP catalyst produced considerably good liquid yield of 47.5% with gasoline content of 77.7%. All the catalysts produced higher gas yield and lower liquid yield with HDPE in comparison to the identical reactions with model plastic mixture.

Hydrocracking reactions with actual waste plastic mixture showed slightly lower conversion, higher liquid yield, and lower gas yield than their corresponding hydrocracking reactions with model plastic mixture. ZC-FP is found the best catalyst with 67.1% liquid yield containing 67.2% of gasoline. ZC-FP has therefore shown potential to be used as a commercial catalyst for the hydrocracking of waste plastics.

Catalyst stability data has revealed that HZSM-5 and its micro-mesoporous catalysts ZC-P, ZC-FP, ZC-F are highly promising catalysts to be reused. The liquid yield of all the catalysts is generally higher when reused without calcining. The calcined-spent catalysts generally showed increased gas production and reduced liquid production than that of their corresponding fresh catalysts.

Declarations

Acknowledgement

The authors acknowledge Higher Education Commission of Pakistan for funding the work under the Project No. 20-2308/NRPU/R&D/HEC/12470. Also, the authors acknowledge Dr. Muhammad Faisal Irfan for providing commercial zeolite beta catalyst.

Funding: Higher Education Commission of Pakistan has funded the work under the Project No. 20-2308/NRPU/R&D/HEC/12470.

Conflicts of interest/Competing interests: There is no conflict of interest.

Availability of data and material: The datasets generated during and/or analysed during the current study are available from the corresponding author on reasonable request.

Code availability: Not applicable

Authors' contributions: Both the authors have significant contribution in the completion of this article.

References

1. Taghiei MM, Feng Z, Huggins FE, Huffman GP (1994) Coliquefaction of waste plastics with coal. Energy Fuels 8:1228–1232
2. Ino H, Matsumoto Y, Takahashi R, Takami K, Nishino J, Itoh M (2008) Aromatization of waste polyolefin pyrolysate over H-ZSM-5 zeolite-supported gallium oxide catalysts. J Mater Cycles Waste Manag 10:129–133
3. Gulab H, Hussain K, Hussain Z, Shah Z (2016) Catalytic co-pyrolysis of Eichhornia Crassipes biomass and polyethylene using waste Fe and $CaCO_3$ catalysts. Int J Energy Res 40:940–951
4. Escola JM, Aguado J, Serrano DP, Briones L (2012) Hydroreforming over Ni/H-beta of the thermal cracking products of LDPE, HDPE and PP for fuel production. J Mater Cycles Waste Manag 14:286–293
5. Williams PT, Bargi R (2004) Hydrocarbon gases and oils from the recycling of polystyrene waste by catalytic pyrolysis. Int J Energy Res 28:31–44
6. Walendziewski J, Steininger M (2001) Thermal and catalytic conversion of waste polyolefines. Catal Today 65:323–330
7. Mosio-Mosiewski J, Warzala M, Morawski I, Dobrzanski T (2007) High-pressure catalytic and thermal cracking of polyethylene. Fuel Process Technol 88:359–364
8. Munir D, Irfan MF, Usman MR (2018) Hydrocracking of virgin and waste plastics: A detailed review. Renew Sust Energ Rev 90:490–515
9. Weitkamp J (2012) Catalytic hydrocracking: Mechanisms and versatility of the process. ChemCatChem 4:292–306
10. Venkatesh KR, Hu J, Tierney JW, Wender I (1995) Hydrocracking of polyolefins to liquid fuels over strong solid acid catalysts. Preprints of Papers, American Chemical Society, Division of Fuel

Chemistry, 788–792
11. Shah N, Rockwell J, Huffman GP (1999) Conversion of waste plastic to oil: direct liquefaction versus pyrolysis and hydroprocessing. Energy Fuels 13:832–838
12. Ding W, Liang J, Anderson LL (1997) Thermal and catalytic degradation of high density polyethylene and commingled post-consumer plastic waste. Fuel Process Technol 51:47–62
13. Ding W, Liang J, Anderson LL (1997) Hydrocracking and hydroisomerization of high-density polyethylene and waste plastic over zeolite and silica-alumina-supported Ni and Ni-Mo sulfides. Energy Fuels 11:1219–1224
14. Feng Z, Zhao J, Rockwell J, Bailey D, Huffman G (1996) Direct liquefaction of waste plastics and coliquefaction of coal-plastic mixtures. Fuel Process Technol 49:17–30
15. Akah A, Hernandez-Martinez J, Garforth J (2013) Enhanced Feedstock Recycling: NovaCrack TM
16. Liu K, Meuzelaar HL (1996) Catalytic reactions in waste plastics, HDPE and coal studied by high-pressure thermogravimetry with on-line GC/MS. Fuel Process Technol 49:1–15
17. Luo M, Curtis CW (1996) Effect of reaction parameters and catalyst type on waste plastics liquefaction and coprocessing with coal. Fuel Process Technol 49:177–196
18. Luo M, Curtis CW (1996) Thermal and catalytic coprocessing of Illinois No. 6. coal with model and commingled waste plastics. Fuel process Technol 49:91–117
19. Ochoa R, Van Woert H, Lee W, Subramanian R, Kugler E, Eklund P (1996) Catalytic degradation of medium density polyethylene over silica-alumina supports. Fuel Process Technol 49:119–136
20. Serrano D, Aguado J, Escola J, Garagorri E, Morselli L, Palazzi G, Orsi R (2004) Feedstock recycling of agriculture plastic film wastes by catalytic cracking. Appl Catal B Environ 49:257–265
21. Hesse ND, White RL (2004) Polyethylene catalytic hydrocracking by PtHZSM-5, PtHY, and PtHMCM-41. J Appl Polymer Sci 92:1293–1301
22. Syamsiro M, Saptoadi H, Norsujianto T, Noviasri P, Cheng S, Alimuddin Z, Yoshikawa K (2014) Fuel oil production from municipal plastic wastes in sequential pyrolysis and catalytic reforming reactors. Energy Procedia 47:180–188
23. Akah A, Hernandez-Martinez J, Rallan C, Garforth AA (2015) Enhanced feedstock recycling of post-consumer plastic waste. Chem Eng Trans 43:2395–2400
24. Isoda T, Maemoto S, Kusakabe K, Morooka S (1999) Hydrocracking of pyrenes over a nickel-supported Y-zeolite catalyst and an assessment of the reaction mechanism based on MD calculations. Energy Fuels 13:617–623
25. Cardona SC, Corma A (2000) Tertiary recycling of polypropylene by catalytic cracking in a semibatch stirred reactor: use of spent equilibrium FCC commercial catalyst. Appl Catal B Environ 25:151–162
26. Munir D, Usman MR (2018) Catalytic hydropyrolysis of a model municipal waste plastic mixture over composite USY/SBA-16 catalysts. J Anal Appl Pyrol 13:44–53
27. Paula TP, Marques MFV, Marques MRC (2019) Influence of mesoporous structure ZSM-5 zeolite on the degradation of urban plastics waste. J Therm Anal Calorim 138:3689–3699

28. Bai R, Song Y, Li Y, Yu J (2019) Creating hierarchical pores in zeolite catalysts. Trends Chem 1:601–611
29. Jia X, Khan W, Wu Z, Choi J, Yip ACK (2019) Modern synthesis strategies for hierarchical zeolites: Bottom-up versus top-down strategies. Adv Powder Technol 30:467–484
30. Mohanraj C, Senthilkumar T, Chandrasekar M (2017) A review on conversion techniques of liquid fuel from waste plastic materials. Int J Energy Res 41:1534–1552
31. Choi SJ, Park Y-K, Jeong K-E, Kim T-W, Chae H-J, Park SH, Jeon J-K, Kim S-S (2010) Catalytic degradation of polyethylene over SBA-16. Korean J Chem Eng 27:1446–1451
32. Munir D, Usman MR (2016) Synthesis and characterization of mesoporous hydrocracking catalysts. IOP Conf Series Mater Sci Eng 146:1–7
33. Munir D, Abdullah, Piepenbreier F, Usman MR (2017) Hydrocracking of a plastic mixture over various micro-mesoporous composite zeolites. Powder Technol 316:542–550
34. Aguado J, Serrano DP, Romero MD, Escola JM (1996) Catalytic conversion of polyethylene into fuels over mesoporous MCM-41. Chem Commun 6:725–726
35. Aguado J, Sotelo JL, Serrano DP, Calles JA, Escola JM (1997) Catalytic conversion of polyolefins into liquid fuels over MCM-41: Comparison with ZSM-5 and amorphous SiO2-Al_2O_3. Energy Fuels 11:1225–1231
36. Munir D, Amer H, Aslam R, Bououdina M, Usman MR (2020) Composite zeolite beta catalysts for catalytic hydrocracking of plastic waste to liquid fuels. Mat Renew Sustain Energy 9:1–9
37. Munir D (2018) Catalytic hydrocracking of waste plastics to liquid fuels. University of the Punjab, Lahore
38. Xia Y, Mokaya R (2004) On the synthesis and characterization of ZSM-5/MCM-48 aluminosilicate composite materials. J Mater Chem 14:863–870
39. Yang Z, Xia Y, Mokaya R (2004) Zeolite ZSM-5 with unique supermicropores synthesized using mesoporous carbon as a template. Adv Mater 16:727–732
40. Boahene PE, Soni KK, Dalai AK, Adjaye J (2011) Application of different pore diameter SBA-15 supports for heavy gas oil hydrotreatment using FeW catalyst. Appl Catal A: General 402:31–40
41. Yoo WC, Zhang X, Tsapatsis M, Stein A (2012) Synthesis of mesoporous ZSM-5 zeolites through desilication and re-assembly processes. Micropor Mesopor Mater 149:147–157
42. Jia L, Sun X, Ye X, Zou C, Gu H, Huang Y, Niu G, Zhao D (2013) Core–shell composites of USY@ Mesosilica: Synthesis and application in cracking heavy molecules with high liquid yield. Micropor Mesopor Mater 176:16–24
43. Huirache-Acuña R, Pawelec B, Rivera-Muñoz E, Nava R, Espino J, Fierro JLG (2009) Comparison of the morphology and HDS activity of ternary Co-Mo-W catalysts supported on P-modified SBA-15 and SBA-16 substrates. Appl Catal B Environ 92:168–184
44. Li H, He S, Ma K, Wu Q, Jiao Q, Sun K (2013) Micro-mesoporous composite molecular sieves H-ZSM-5/MCM-41 for methanol dehydration to dimethyl ether: Effect of SiO_2/Al_2O_3 ratio in H-ZSM-5. Appl

Catal A: General 450:152–159

45. Mouli KC, Soni K, Dalai A, Adjaye J (2011) Effect of pore diameter of Ni–Mo/Al-SBA-15 catalysts on the hydrotreating of heavy gas oil. Appl Catal A: General 404:21–29
46. Klimova T, Lizama L, Amezcua J, Roquero P, Terrés E, Navarrete J, Domínguez J (2004) New NiMo catalysts supported on Al-containing SBA-16 for 4, 6-DMDBT, hydrodesulfurization: Effect of the alumination method. Catal Today 98:141–150
47. Gallo JMR, Bisio C, Marchese L, Pastore HO (2008) Surface acidity of novel mesostructured silicas with framework aluminum obtained by SBA-16 related synthesis. Microporous Mesoporous Mater 111:632–635
48. Sun H, Tang Q, Du Y, Liu X, Chen Y, Yang Y (2009) Mesostructured SBA-16 with excellent hydrothermal, thermal and mechanical stabilities: Modified synthesis and its catalytic application. J Colloid Interf Sci 333:317–323
49. Shah T, Lia B, Abdalla ZEA (2009) Direct synthesis of Ti-containing SBA-16-type mesoporous material by the evaporation-induced self-assembly method and its catalytic performance for oxidative desulfurization. J Colloid Interf Sci 336:707–711
50. Orr EC, Tuntawiroon W, Ding WB, Bolat E, Rumple S, Eyring EM, Anderson LL (1995) Thermal and catalytic coprocessing of coal and waste materials. Prepr Am Chem Soc Div Fuel Chem 40:44–50
51. Zmierczak W, Xiao X, Shabtai J (1996) Depolymerization-liquefaction of plastics and rubbers. 2. Polystyrenes and styrene-butadiene copolymers. Fuel Process Technol 49:31–48
52. Shabtai J, Xiao X, Zmierczak W (1997) Depolymerization-liquefaction of plastics and rubbers. 1. Polyethylene, polypropylene, and polybutadiene. Energy Fuels 11:76–87
53. Ding WB, Liang J, Anderson LL (1997) Hydrocracking of waste plastics to clean liquid fuels. Prepr Am Chem Soc Div Fuel Chem 42:1008–1013
54. Ramdoss PK, Tarrer AR (1998) High-temperature liquefaction of waste plastics. Fuel 77:293–299
55. Williams PT, Slaney E (2007) Analysis of products from the pyrolysis and liquefaction of single plastics and waste plastic mixtures. Resour Conserv Recy 51:754–769

Figures

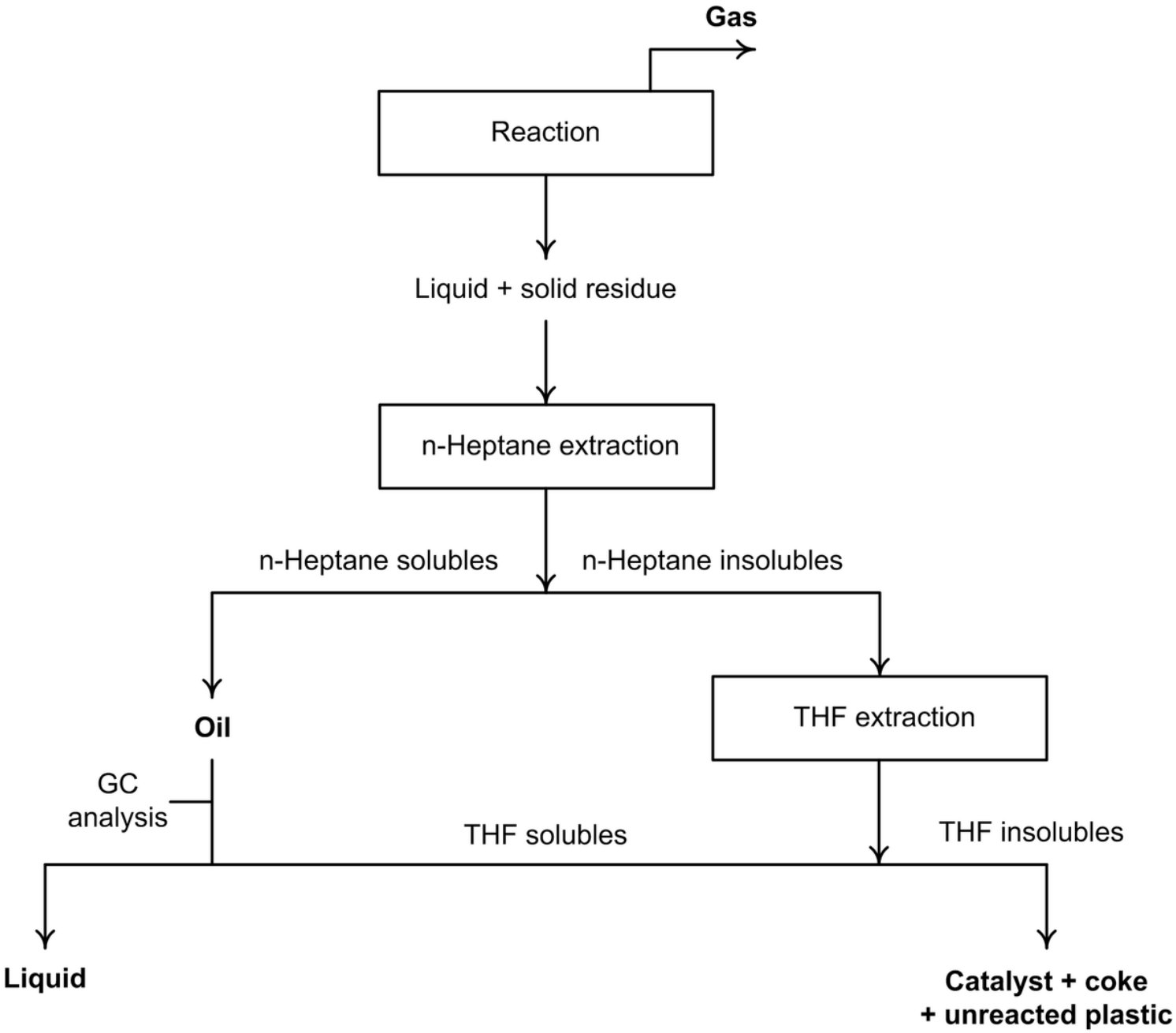

Figure 1

Analysis scheme for the reaction products.

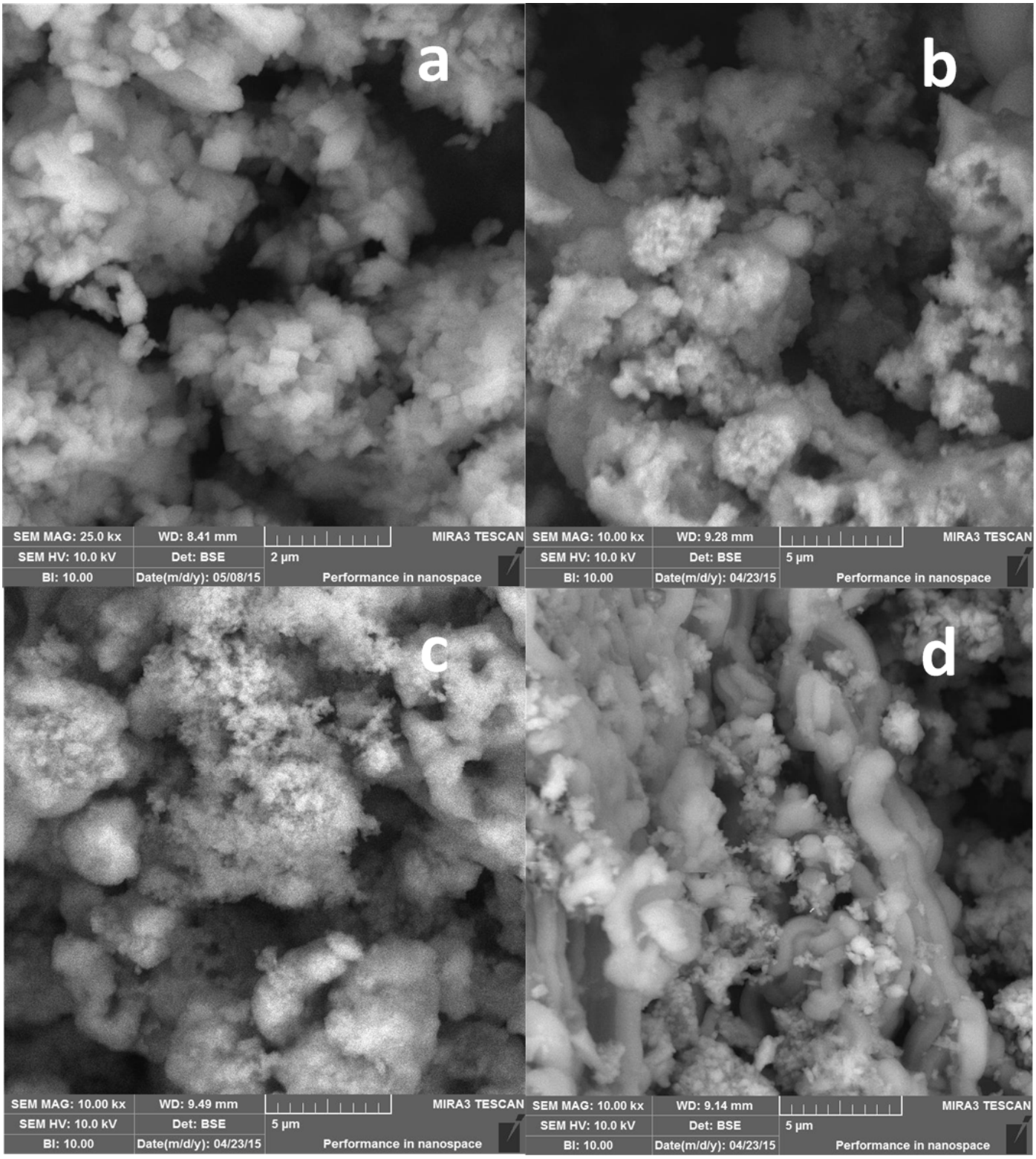

Figure 2

SEM images of the micro-mesoporous HZSM-5 catalysts: a) HZSM-5, b) ZC-F, c) ZC-FP, and d) ZC-P.

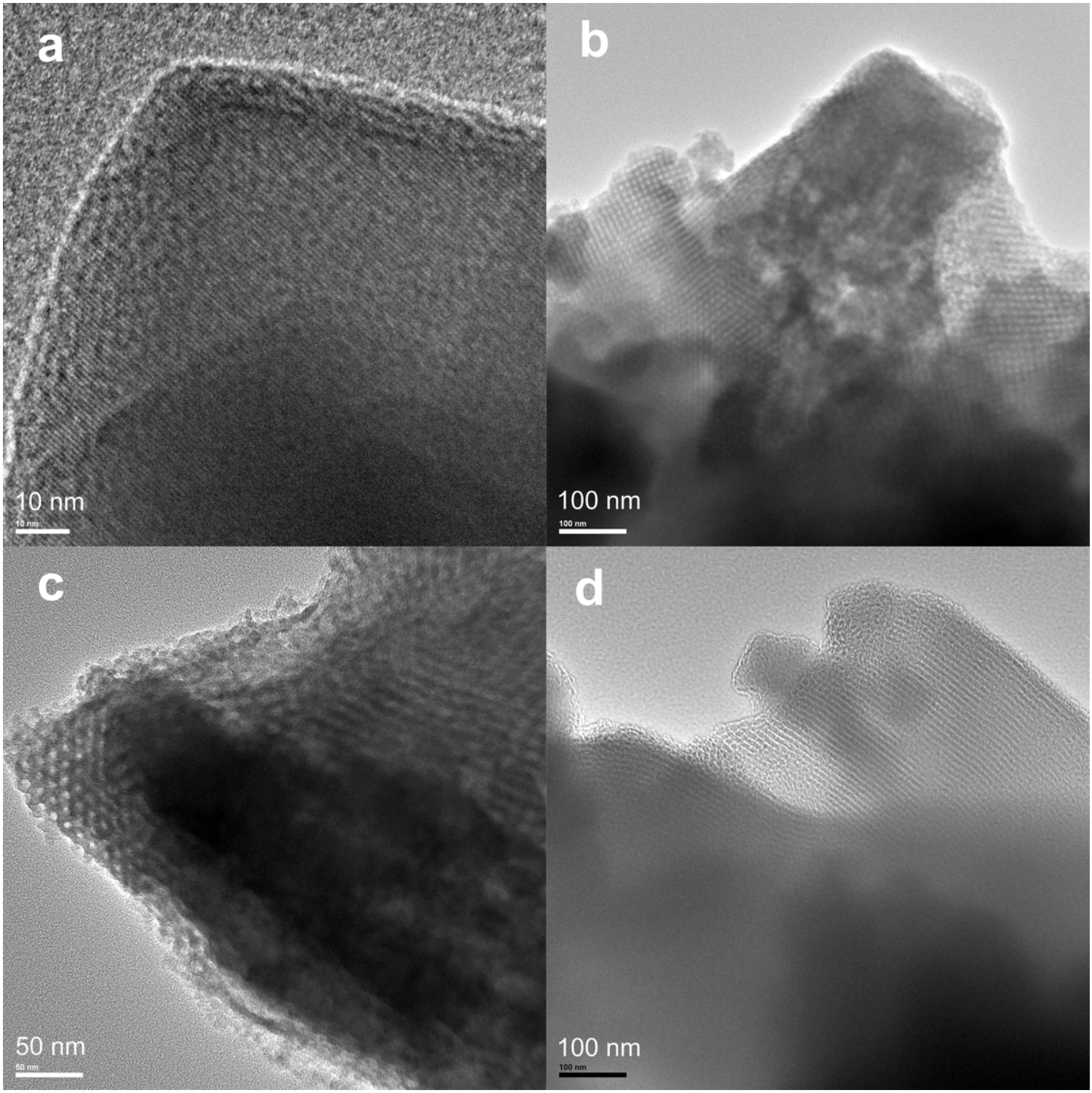

Figure 3

TEM images of the micro-mesoporous HZSM-5 catalysts: a) HZSM-5, b) ZC-F, c) ZC-FP, and d) ZC-P.

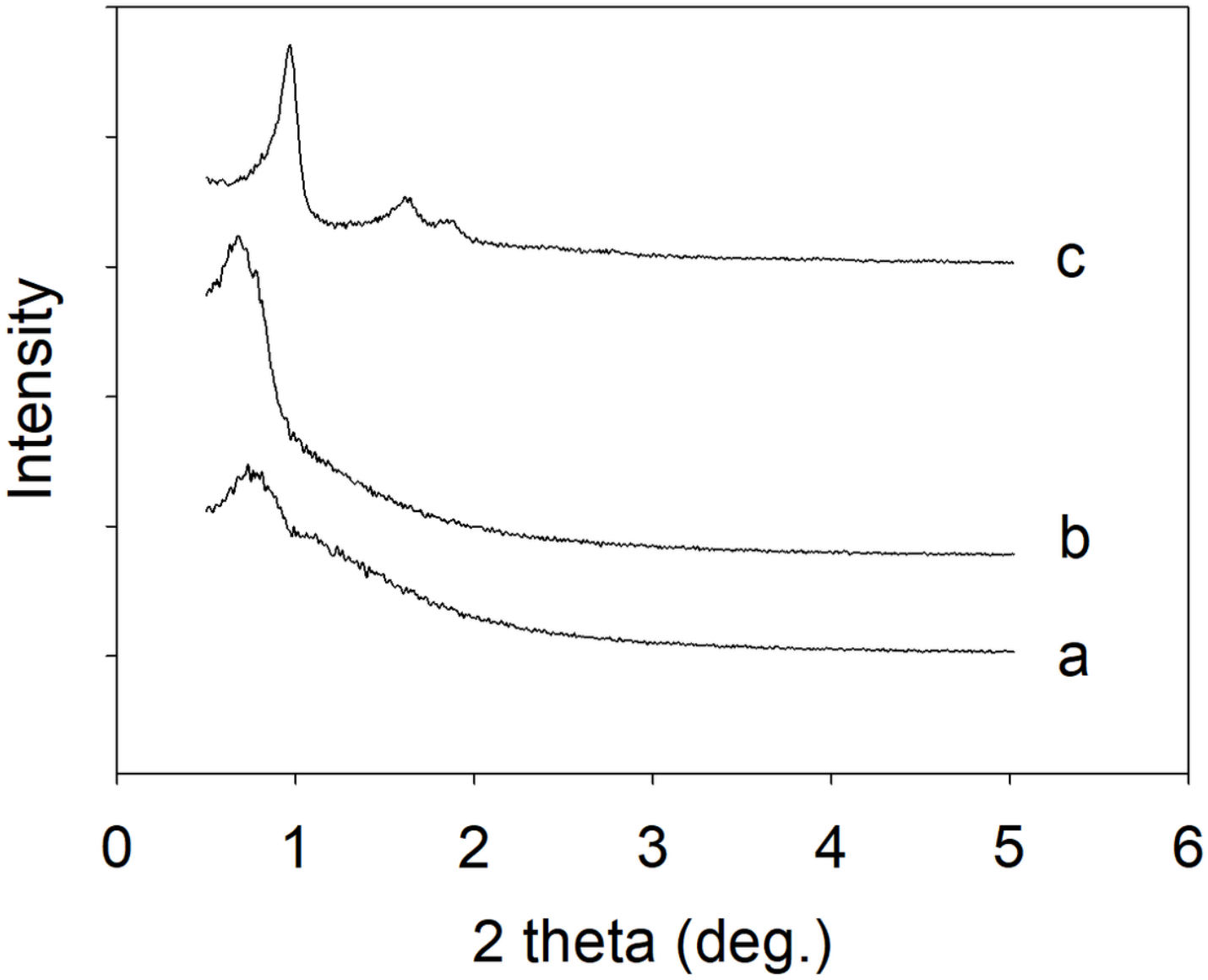

Figure 4

Small angle XRD patterns of the micro-mesoporous HZSM-5 catalysts: (a) ZC-F, (b) ZC-FP, and (c) ZC-P.

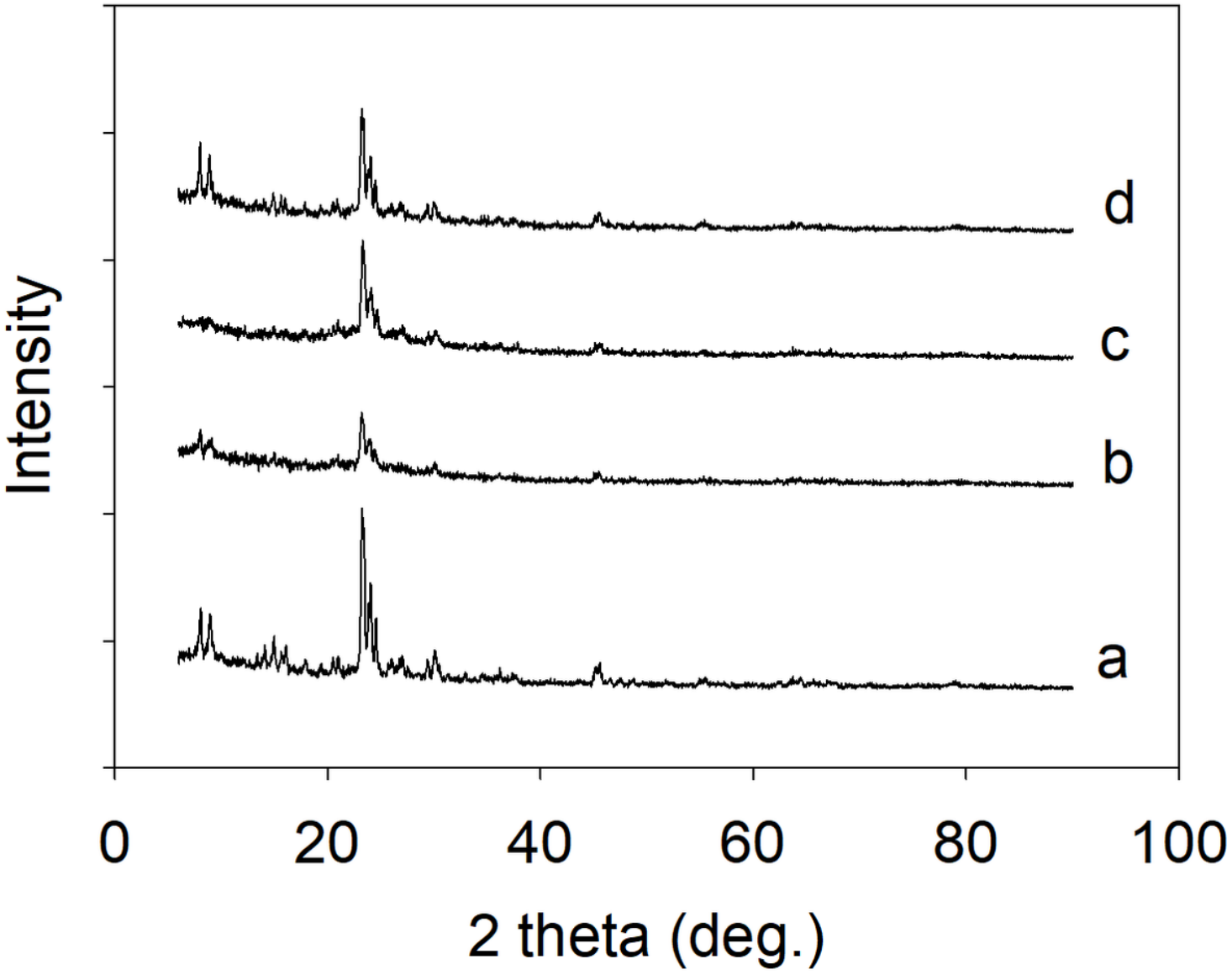

Figure 5

Wide angle XRD diffraction patterns of the micro-mesoporous HZSM-5 catalysts: (a) HZSM-5, (b) ZC-F, (c) ZC-FP, and (d) ZC-P.

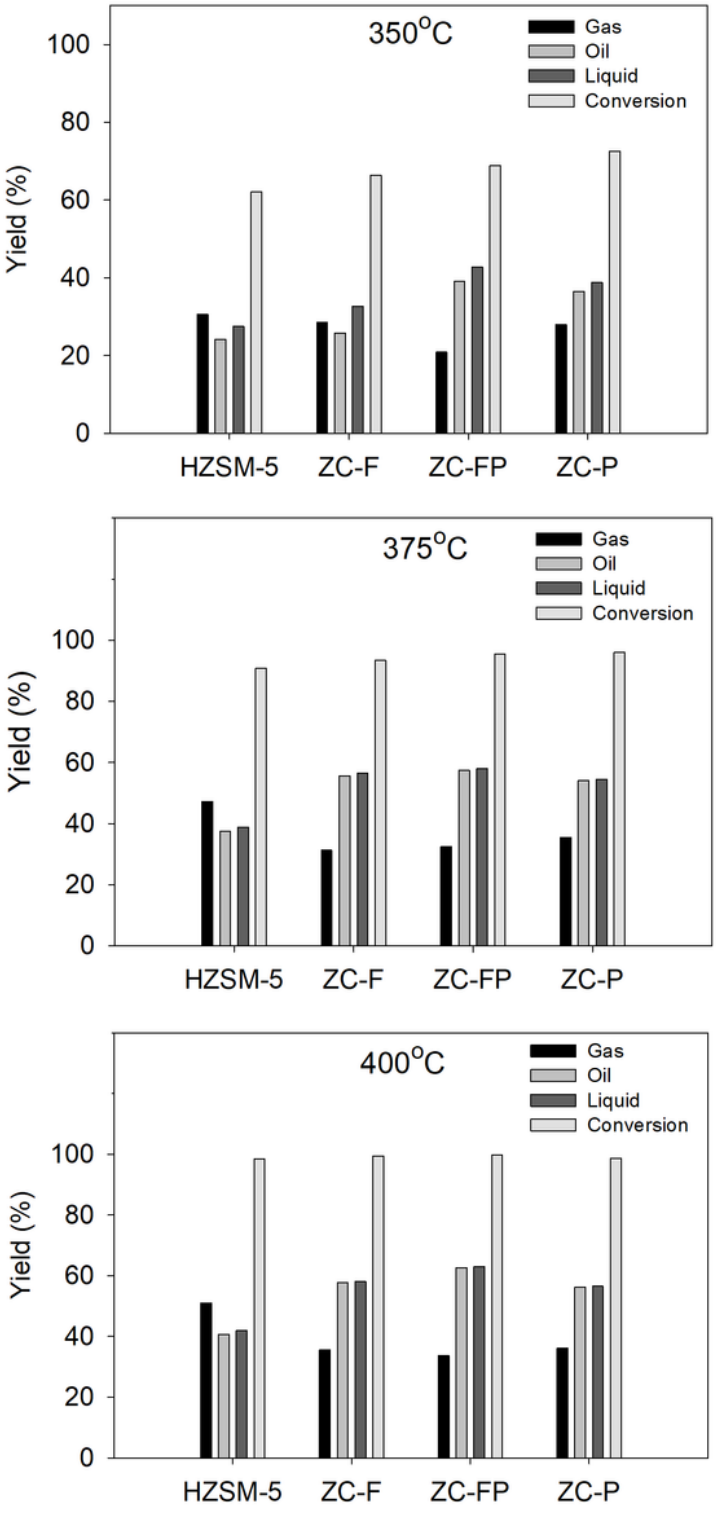

Figure 6

Results of the hydrocracking of model plastic mixture over the micro-mesoporous HZSM-5 catalysts. 500 ml autoclave reactor, 20 bar initial cold hydrogen pressure, 60 min residence time, and 20:1 feed to catalyst ratio (by weight).

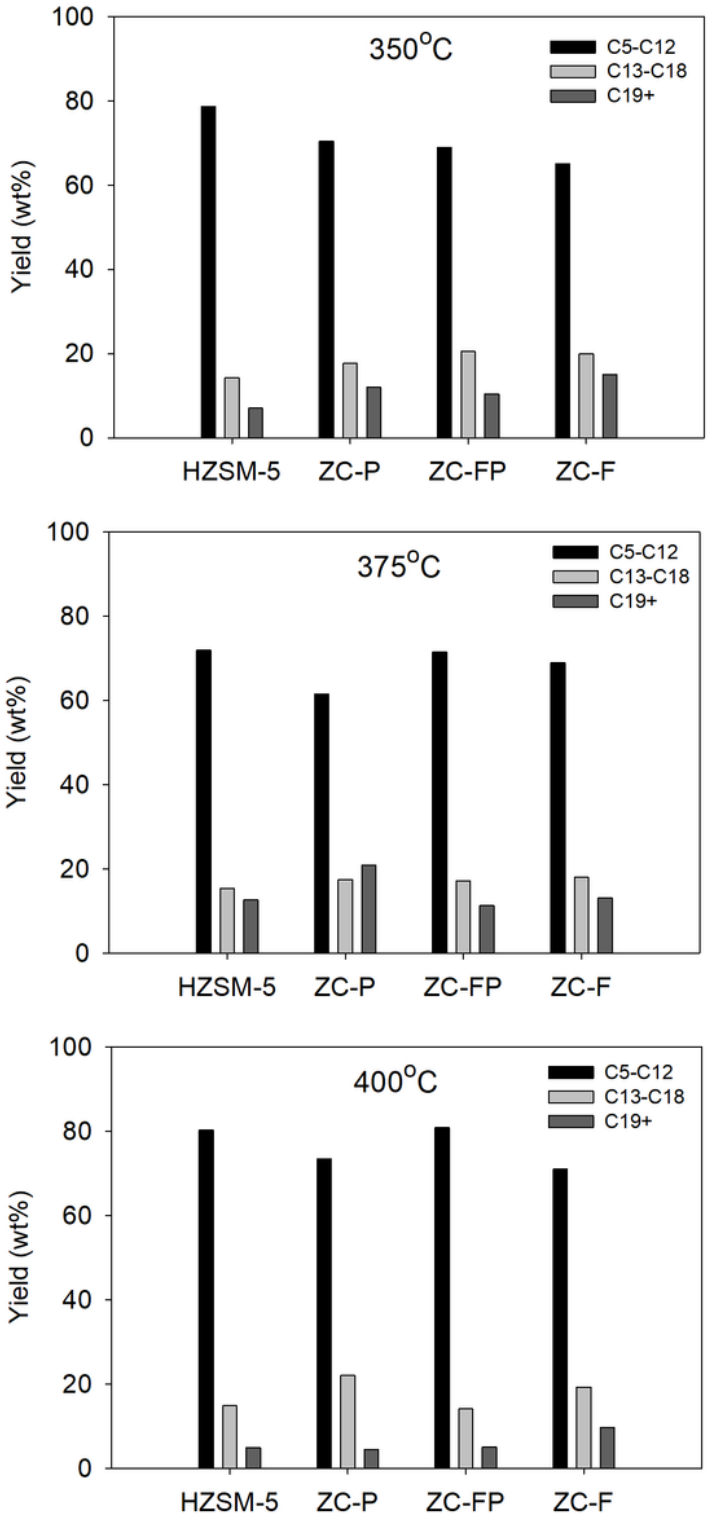

Figure 7

Results of the GC analysis of the n-heptane soluble liquids obtained by the hydrocracking of model plastic mixture over the micro-mesoporous HZSM-5 catalysts. 500 ml autoclave reactor, 20 bar initial cold hydrogen pressure, 60 min residence time, and 20:1 feed to catalyst ratio (by weight).

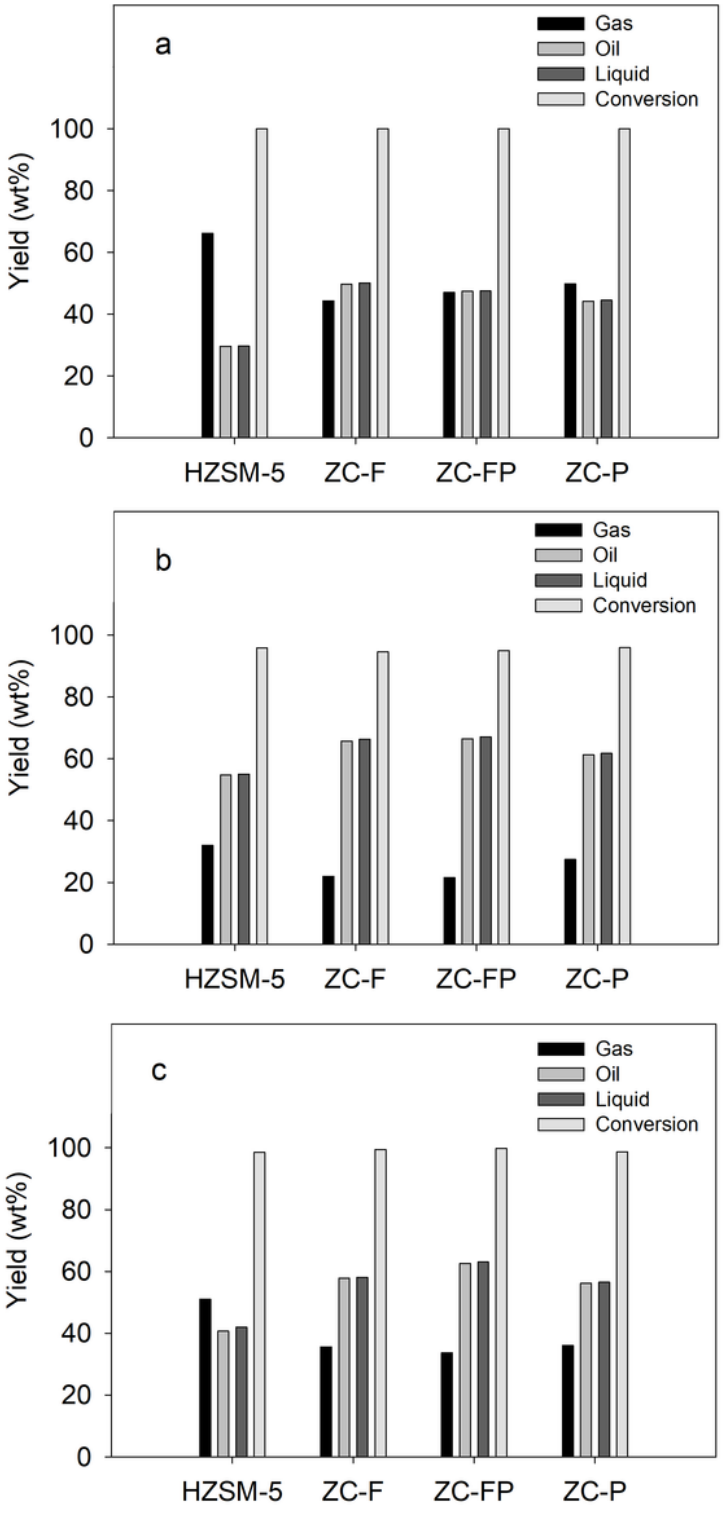

Figure 8

Results of the hydrocracking reaction over the micro-mesoporous HZSM-5 catalysts with: a) HDPE, b) Waste Plastic, and c) Model plastic mixture. 500 ml autoclave reactor, 400 °C temperature, 20 bar cold hydrogen pressure, 60 min residence time, and 20:1 feed to catalyst ratio (by weight).

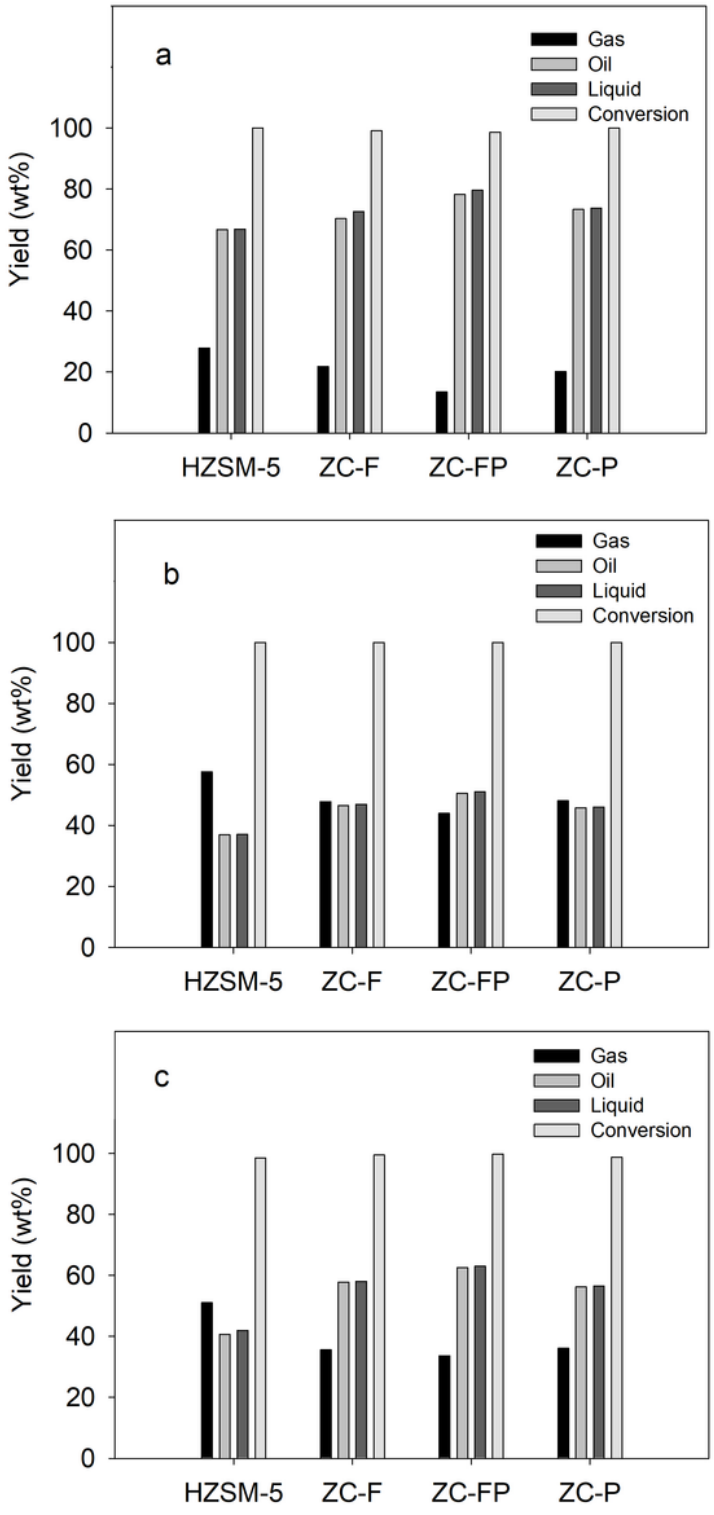

Figure 9

Results of the hydrocracking of model plastic mixture over the micro-mesoporous HZSM-5 catalysts: a) Dried spent catalysts, b) Calcined spent catalysts, and c) Fresh catalysts. 500 ml autoclave reactor, 400 °C temperature, 20 bar cold hydrogen pressure, 60 min residence time, and 20:1 feed to catalyst ratio (by weight).

Supplementary Files

This is a list of supplementary files associated with this preprint. Click to download.

- Munir18Mar2021SupplementaryMaterial.docx